JOURNAL OF THE ROYAL SOCIETY Interface

Cryoprotection–lyophilization and physical stabilization of rifampicin-loaded flower-like polymeric micelles

Marcela A. Moretton, Diego A. Chiappetta and Alejandro Sosnik

J. R. Soc. Interface 2012 **9**, 487-502 first published online 24 August 2011
doi: 10.1098/rsif.2011.0414

JOURNAL OF THE ROYAL SOCIETY Interface

J. R. Soc. Interface (2012) **9**, 487–502
doi:10.1098/rsif.2011.0414
Published online 24 August 2011

Cryoprotection–lyophilization and physical stabilization of rifampicin-loaded flower-like polymeric micelles

Marcela A. Moretton[1,2], Diego A. Chiappetta[1,2] and Alejandro Sosnik[1,2,*]

[1]*The Group of Biomaterials and Nanotechnology for Improved Medicines (BIONIMED), Department of Pharmaceutical Technology, Faculty of Pharmacy and Biochemistry, University of Buenos Aires, Buenos Aires 1113, Argentina*
[2]*National Science Research Council (CONICET), Buenos Aires, Argentina*

Rifampicin-loaded poly(ε-caprolactone)–*b*-poly(ethylene glycol)–poly(ε-caprolactone) flower-like polymeric micelles display low aqueous physical stability over time and undergo substantial secondary aggregation. To improve their physical stability, the lyoprotection–lyophilization process was thoroughly characterized. The preliminary cryoprotectant performance of mono- and disaccharides (e.g. maltose, glucose), hydroxypropyl-β-cyclodextrin (HPβCD) and poly(ethylene glycol) (PEG) of different molecular weights was assessed in freeze–thawing assays at −20°C, −80°C and −196°C. The size and size distribution of the micelles at the different stages were measured by dynamic light scattering (DLS). A cryoprotectant factor (f_c) was determined by taking the ratio between the size immediately after the addition of the cryoprotectant and the size after the preliminary freeze–thawing assay. The benefit of a synergistic cryoprotection by means of saccharide/PEG mixtures was also assessed. Glucose (1 : 20), maltose (1 : 20), HPβCD (1 : 5) and glucose or maltose mixtures with PEG3350 (1 : 20) (copolymer:cryoprotectant weight ratio) were the most effective systems to protect 1 per cent micellar systems. Conversely, only HPβCD (1 : 5) cryoprotected more concentrated drug-loaded micelles (4% and 6%). Then, those micelle/cryoprotectant systems that displayed f_c values smaller than 2 were freeze-dried. The morphology of freeze-dried powders was characterized by scanning electron microscopy and atomic force microscopy and the residual water content analysed by the Karl Fisher method. The HPβCD-added lyophilisates were brittle porous cakes (residual water was between 0.8% and 3%), easily redispersable in water to form transparent systems with a minimal increase in the micellar size, as determined by DLS.

Keywords: rifampicin-loaded flower-like polymeric micelles; cryoprotection/lyophilization; physical stabilization

1. INTRODUCTION

Tuberculosis (TB) is the second most deadly infection next to the human immunodeficiency virus (HIV) [1,2]. Approximately 2 billion people are infected with *Mycobacterium tuberculosis* [3], although the disease develops mainly in immune-compromised patients. TB is endemic in emerging nations and belongs to the group of so-called poverty-related diseases [4]. In addition, a resurgence of the disease has been observed in the developed world over the last two decades, mainly associated with the HIV epidemic [5]. The annual TB mortality is approximately 1.7 million people [6]. Owing to the high prevalence of HIV/TB co-infection, the World Health Organization (WHO) declared a global sanitary emergency in 1993 [7].

The gold standard pharmacotherapy comprises a first phase (two months) with four drugs (rifampicin, RIF; isoniazide, INH; pyrazinamide and ethambutol) with a second phase (four months) with RIF and INH [8,9]. The non-resistant form of TB is curable, although it represents 25 per cent of preventable deaths worldwide [4,10]. Patient compliance and adherence are low owing to frequent and prolonged administration schedules, leading to treatment cessation and, often, the development of resistant strains [11].

RIF is the most potent anti-TB drug [12]. A complex combination of molecular features such as high molecular weight (823 Da), amphotericity (pK_{a1} in diluted water is 1.7, pK_{a2} in diluted water is 7.9 and the isoelectric point is 4.8) [13] and amphiphilicity challenges the development of pharmaceutical formulations [14] (scheme 1). Its intrinsic pH-dependent aqueous solubility ranges between 1 and 3 mg ml^{-1} [15]. RIF has been classified as class II of the Biopharmaceutic

*Author for correspondence (alesosnik@gmail.com).

Received 27 June 2011
Accepted 26 July 2011

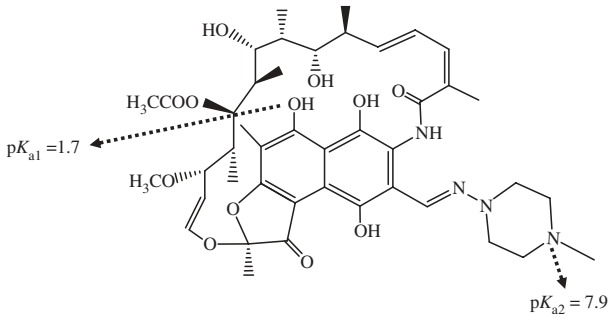

Scheme 1. Rifampicin structure. The pK_{a1} (in water) has been attributed to the hydroxyl moiety at C-8, while the pK_{a2} (in water) has been attributed to N-4 of piperazine.

Classification System [16], although its reclassification as class IV has been recommended [17]. Under gastric conditions, RIF is gradually hydrolysed to the non-active form 3-formyl RIF SV. This degradation pathway is hastened by INH [18,19]; the co-administration of RIF/INH in fixed dose combinations is employed to prevent mono-therapy [20]. The WHO has raised awareness of the reduced oral bioavailability of RIF in these formulations [21]. Considering the limited pace of new drug development and their greater cost, there is an urgent need to investigate versatile technologies to optimize TB pharmacotherapy [22–24].

We previously investigated the molecular implications of RIF encapsulation within 'flower-like' polymeric micelles made of poly(ϵ-caprolactone)–*b*-poly(ethylene glycol)–poly(ϵ-caprolactone) (PCL–PEG–PCL) block copolymers [25]. This unique kind of structure is generated by the aggregation of amphiphilic ABA copolymers that combine two terminal hydrophobic A segments (e.g. PCL) with a central hydrophilic B one (e.g. PEG). The looped hydrophilic corona of the PEG block confers on the system the appearance of flower petals. The overall micellar size appears to be the key structural parameter dictating the encapsulation capacity of the micelles; smaller polymeric micelles (e.g. poly(ethylene oxide)–poly(propylene oxide)–poly(ethylene oxide), PEO–PPO [26]) did not improve the solubility of the drug [27]. Owing to the limited aqueous solubility of PEG–PCL copolymers, the maximum concentration employed to produce the micelles is usually 1–2%. In our previous study, we explored concentrations as high as 6 per cent [25]. The RIF aqueous solubility was increased up to 5.4 times, this performance being better than that of cyclodextrins [28] and mannose-grafted poly(propyleneimine) dendrimers [29]. Independently of the copolymer molecular weight, the PEG/PCL molar ratio and its concentration, drug-free micelles display a relatively low physical stability [25,30]. Owing to its amphotericity, RIF imposes an additional deleterious effect on the physical stability of the system [25]. This phenomenon results in a relatively fast size enlargement and copolymer and drug precipitation. Thus, the lyophilization of RIF-loaded systems would appear to be an unavoidable stage to optimize their physical stability in the mid- to long term [30].

Lyophilization is the sublimation of water from a frozen sample and it comprises (i) freezing, (ii) primary drying, and (iii) secondary drying. This process has been extensively investigated to stabilize a broad variety of lipid and polymeric drug nanocarriers [31]. Nevertheless, there have been only a few reports on the successful lyophilization of drug-free [30] and drug-loaded PCL–PEG and poly(lactic acid)–PEG polymeric micelles [32–34]; the systems evaluated were highly diluted (less than or equal to 3%). The different steps of the process entail freezing, dehydration and mechanical stresses that can destabilize the micelles and lead to secondary aggregation and fusion [31]. Lyophilization of more concentrated micellar dispersions is even more challenging. The use of cryoprotectants in relatively high concentrations (10–30%) is generally required [30]. Interestingly, data on the effectiveness or not of a certain cryoprotectant are contradictory and strongly depend on the conditions of the lyophilization. Also, very slight changes in (i) the composition of the system or (ii) the properties of the encapsulated drug can affect the efficiency of the process. Since micelles are more dynamic systems than solid polymeric nanoparticles and display a greater re-aggregation tendency, their lyophilization is even more complex [35].

This work comprehensively investigated and characterized the cryoprotection/lyophilization of RIF-loaded flower-like micelles. The efficient cryoprotection of relatively concentrated PCL-containing drug-loaded micelles (4–6%) is reported for the first time.

2. MATERIAL AND METHODS

2.1. Materials

Poly(ethylene glycol) of molecular weights 3.35 kDa (PEG3350), 6 kDa (PEG6000) and 10 kDa (PEG10 000) was supplied by Merck Chemicals (Argentina). PEG10 000 for the synthesis of PCL–PEG–PCL copolymers was dried under vacuum (100–120°C in an oil bath for 2 h) before use. Epsilon-caprolactone 99 per cent (monomer, CL; Sigma-Aldrich, USA), tin (II) 2-ethylhexanoate 95 per cent (catalyst, SnOct; Sigma-Aldrich), RIF 98.2 per cent (Parafarm, Argentina) and solvents of analytical grade were used as received. D-(+) maltose and D-(+) glucose were supplied by Sigma-Aldrich. Hydroxypropyl-β-cyclodextrin (HPβCD) (CavasolW7 HP Pharma, Wacker Chemie AG, Germany) was donated by ISP Technologies Inc. (Argentina).

2.2. Copolymer synthesis

PCL–PEG–PCL copolymers were synthesized by means of a microwave-assisted ring opening polymerization of CL initiated by PEG10 000 in the presence of SnOct [25,36,37]. Briefly, PEG10 000 was poured into a round-bottom flask and dried (see above). Then, CL (10% in molar excess) and SnOct (1 : 40 molar ratio to CL) were added. The round-bottom flask was placed in the centre of the microwave oven (Itedo, Japan, radiation frequency 2.45 GHz, maximum operating power 800 W) and the reaction mixture was exposed to microwave irradiation. The crude product was dissolved in dichloromethane (50 ml) and precipitated in petroleum ether at 35–65°C (500 ml). The cleaning procedure was

repeated once more. The precipitate was isolated by filtration, washed several times with petroleum ether, dried until constant weight at room temperature and stored at −20°C until use. Two PCL–PEG–PCL derivatives displaying terminal PCL segments with average molecular weight of 3.7 kDa (32 CL units per arm) and 4.5 kDa (40 CL units per arm) and theoretical molecular weights of 17.4 and 19.0 kDa, respectively, were synthesized. PCL3700–PEG10 000–PEG3700 and PCL4500–PEG10 000–PCL4500 copolymers are denominated PCL(3700) and PCL(4500), respectively. The CL/EO molar ratio and the number average molecular weight (M_n) were determined from proton nuclear magnetic resonance (^{1}H-NMR) spectra, and number and weight average molecular weights (M_n and M_w) and molecular weight distributions (M_w/M_n polydispersity index; PDI) were determined by gel permeation chromatography (GPC) [25]. These copolymers were selected because they showed the best RIF encapsulation performance of all the derivatives evaluated [25].

2.3. Preparation of RIF-loaded PCL–PEG–PCL micelles

RIF-loaded micelles of copolymer concentrations between 1 and 6 per cent w/v were prepared by means of the co-solvent–evaporation method, as depicted elsewhere [25]. Briefly, RIF and the corresponding copolymer amount were co-solubilized in acetone (11 ml) and added drop-wise to water (10 ml) under mechanical stirring (three-blade propeller, 1060 r.p.m.) using a programmable syringe infusion pump (PC11UB, Apema, Argentina) over 20 min. Samples were maintained under mechanical stirring over 1 h and filtered (0.45 µm cellulose nitrate membranes, Whatman GmbH, Germany). RIF concentrations were determined by UV (340 nm, Cary [1E] UV–Visible Spectrophotometer Varian, USA), at 25°C; a calibration curve of RIF in DMF covering the range between 5.5 and 33.2 µg ml^{-1} (the correlation factor was 0.9995–0.9999) was used. RIF-free micelles employed in thermal analysis were prepared following the same procedure, though without the addition of the drug. The RIF payload (±s.d.) in each micellar system is presented in table 1 ($n = 3$).

2.4. Freeze–thawing study of RIF-loaded micelles

RIF-loaded micelles (1 ml) were frozen at different freezing rates (−20°C, −80°C and −196°C) with different amounts of cryoprotectant, stored for 48 h at the freezing temperature, and finally thawed at room temperature. Preliminary effective cryoprotection was considered when the systems did not present macroscopic aggregates and remained totally translucent to the naked eye. The size and size distribution before and after the freeze–thawing process of samples containing the cryoprotectant were measured by dynamic light scattering (DLS; see below). The cryoprotection factor (f_c) was calculated according to

$$f_c = \frac{S_f}{S_i},$$

Table 1. RIF payloads in PCL–PEG–PCL micelles with a copolymer concentration between 1% and 6% (w/v) ($n = 3$).

copolymer concentration (%w/v)	RIF concentration (mg ml^{-1}) (±s.d.)	
	PCL(3700)	PCL(4500)
1	4.8 (0.04)	4.7 (0.05)
4	9.8 (0.15)	10.0 (0.21)
6	11.8 (0.10)	12.0 (0.06)

where S_i and S_f are the size immediately after the addition of the cryoprotectant and the size after the freeze–thawing treatment, respectively. RIF-loaded micelles deprived of cryoprotectant were used as controls. When an f_c value lower than 2.0 was registered, the cryoprotection system was considered efficient and selected for the lyophilization process [38].

For sugar/PEG3350 cryoprotectant combinations, additivity of their properties was assumed and the glass transition temperature of the maximally freeze-concentrated fraction (T'_g) [39] of the mixture was estimated from the Fox equation [40]

$$\frac{1}{T'_g} = \frac{W_1}{T'_{g1}} + \frac{W_2}{T'_{g2}},$$

where W_1 and W_2 are the weight fractions and T'_{g1} and T'_{g2} are the glass transition temperatures of the sugar and the PEG3350, respectively.

2.5. Lyophilization of RIF-loaded micelles

Those samples that withstood the freeze–thawing assay were poured (1 ml) into glass vials, frozen at the corresponding temperature and lyophilized (freeze-dryer FIC-L05, FIC, Scientific Instrumental Manufacturing, Argentina). The temperatures of the freeze-dryer shelf and the condenser were −14°C and −40°C, respectively, and the pressure was 0.03 mbar. Then, samples were resuspended in the original volume of water and the efficiency of the cryo/lyoprotection provided by each additive was established following the procedure described above for the freeze–thawing assays. Cryo/lyoprotectant-free systems were used as controls.

2.6. Thermal analysis upon lyophilization

The thermal behaviour of different unloaded and RIF-loaded micelles that were lyophilized without and with cryoprotectant was analysed by differential scanning calorimetry (DSC; Mettler Toledo TA-400 differential scanning calorimeter, USA). Samples (2.0–10.5 mg) were sealed in 40 µl Al crucible pans (Mettler ME-27 331, Switzerland) and heated from 25°C to 300°C at 10°C min^{-1} under a nitrogen atmosphere. An empty pan was used as a reference. Pristine and lyophilized RIF were analysed for comparison. The parameters that were determined were: (i) the melting temperature (T_m) and the enthalpy of fusion (ΔH_m) of the copolymer, (ii) the dehydration temperature (T_{deh}), and (iii) the decomposition temperature (T_{decomp}) of RIF and HPβCD. ΔH values were

normalized by taking the ratio between the absolute value and the relative copolymer content in the sample.

To assess the T_g' of HPβCD and relate this to the cryo/lyoprotectant efficacy, a highly concentrated aqueous solution (30%) was analysed by DSC (Mettler Toledo 822, USA). The HPβCD sample (16.91 mg) was quenched to −100°C and then heated up to 25°C (10°C min^{-1}). The T_g' was calculated at the temperature at which the change in the specific heat begins.

2.7. Measurement of micellar size, size distribution and zeta potential

The size and size distribution of the different drug-loaded micelles (i) immediately after preparation, (ii) on addition of the cryoprotectant, (iii) during the freeze–thawing assay, and (iv) during the lyophilization were measured by DLS (Zetasizer Nano-Zs, Malvern Instruments, UK) provided with a 4 mW He–Ne (633 nm) laser and a digital correlator ZEN3600, at 25°C. Measurements were conducted at a scattering angle of $\theta = 173°$ to the incident beam. Samples were equilibrated at 25°C for at least 30 min prior to the analysis. In the case of lyophilized systems, the analysis was conducted immediately after reconstitution in the volume of water required to obtain the original concentration. To reconstitute these specimens, the corresponding volume of water was added to the dry powder, vortexed for 1 min and hand-shaken for an additional 2 min. Data were processed using CONTIN algorithms (Malvern Instruments), based on the theory of Brownian motion and the Stocks–Einstein equation [41]

$$D = \frac{k_B T}{3\pi\eta d_h},$$

where D is the diffusion coefficient, k_B is the Boltzmann constant, T is the temperature and η is the solvent viscosity. Results of the hydrodynamic diameter (D_h) and PDI are expressed as the average of at least five measurements. The same technique was used to measure zeta potential values of cryoprotected drug-loaded micelles before and after lyophilization.

2.8. Field emission gun scanning electron microscopy

The morphology of RIF-loaded micelles lyophilized with or without HPβCD was characterized by means of field emission gun scanning electron microscopy (FEG-SEM; Zeiss Supra 40 apparatus Gemini column, Germany) operated at 3.0 kV accelerating voltage. Samples were previously coated with gold using a sputter coating method. The thickness of the gold layer was between 5 and 10 nm.

2.9. Atomic force microscopy

A complementary morphological analysis was conducted by means of atomic force microscopy (AFM; NanoScope III_a-Quadrex Atomic Force Microscope, Digital-Veeco, USA). HPβCD (50 mg) was added to fresh 1 per cent RIF-loaded micelles of PCL(4500) copolymer (1 ml) and analysed. An identical sample was frozen at −196°C, lyophilized and analysed. An appropriate dilution of the micellar system was placed on the surface of a clean mica wafer and dried under nitrogen flow at room temperature. AFM observations were performed with a 20 μm scanner in a tapping mode under a nitrogen atmosphere. Data were processed with WSxM 4.0 Beta 3.1 scanning probe microscopy software (Nanotec Electrónica S.L., Spain) [42].

2.10. Determination of residual water

The residual water in the different lyophilized samples was determined by the Karl Fisher method (Mettler Karl Fisher titrator DL18, Mettler-Toledo, Switzerland) using the CombiTitrant 5 one-component reagent (Merck, Germany), following the supplier's instructions. Results are expressed as the mean ± s.d. ($n = 3$).

2.11. Physico-chemical stability of lyophilized samples

To evaluate the physico-chemical stability of the lyophilized systems, dry specimens were stored at −20°C and 25°C over one month. The parameters $f'_{c-20°C}$ and $f'_{c25°C}$ were calculated from the following equation:

$$f_c' = \frac{S_f'}{S_i'},$$

where S_i' and S_f' are the micellar size immediately after reconstitution at day 0 of lyophilization and the size after one month of storage at −20°C or 25°C, respectively. In parallel, the concentration of RIF was determined by high-performance liquid chromatography (HPLC; see below).

2.12. High-performance liquid chromatography instrumentation

The stability of RIF after the lyophilization was analysed by HPLC. The HPLC (Thermo Scientific, USA) system consisted of a Spectra System P4000 quaternary gradient pump, a Spectra System AS3000 variable volume autosampler, a Spectra System UV2000 UV-visible dual wavelength detector ($\lambda = 254$ nm) and a Spectra System SCM1000 solvent degasser. The analysis was carried out on a reverse-phase HPLC using a SunFire C18 column (150 × 4.6 mm i.d., particle size 5 μm, Waters, Ireland) and a mobile phase methanol: phosphate buffer pH 6.8 (63 : 37). The flow rate was maintained at 1 ml min^{-1}, the injection volume was 20 μl and the elution time was 18 min. The validation range was 6.25–100 μg ml^{-1}. Data were acquired using Thermo Scientific ChromQuest 5.0 software.

3. RESULTS AND DISCUSSION

3.1. Freeze–thawing

Freezing is the first and the most critical step in colloidal nanoparticle lyophilization. During this step, the system separates into multiple phases. One phase is composed of ice, while the other contains the nanoparticles, the cryoprotectants, free drug and other added pharmaceutical excipients [31]. Destabilizing stresses, such as the increase in nanoparticle

Table 2. List of cryoprotectants evaluated in the freeze–thawing assay of RIF-loaded PCL–PEG–PCL polymeric micelles with their respective T'_g values.

cryoprotectant	cryoprotection mechanism	concentration (%w/v)	T'_g (°C)
pristine cryoprotectant			
maltose	glassy/vitreous matrix containing immobile nanoparticles	5, 10, 20	−29.5[a]
glucose		5, 10, 20	−45.0[a]
HPβCD		5, 10, 20, 30	−13.9[b], −14.8[c]
sorbitol		5, 10, 20	−43.9[d]
PEG3350	steric hindrance	1, 2, 5	−62.0[e]
PEG6000		1, 2, 5	
PEG10 000		0.5, 1.5	
cryoprotectant mixtures			
glucose/PEG3350	combined mechanism	5/5[f], 10/10[f]	−52.1[g]
maltose/PEG3350		10/10[f]	−40.0[g]

[a]Obtained from Miyajima [45].
[b]Determined by DSC.
[c]Obtained from Abdelwahed *et al.* [40].
[d]Obtained from Saez *et al.* [38].
[e]Obtained from Heller *et al.* [46].
[f]5/5, the cryoprotection mixture comprised 5% glucose and 5% PEG3350; 10/10, the cryoprotection mixture comprised 10% glucose and 10% PEG3350 or 10% maltose and 10% PEG3350.
[g]Calculated by the Fox equation.

concentration in one phase and the formation of aggregates [43], or physical stresses related to the freezing of the solution might appear.

One of the formulation key features is the glass transition temperature of the maximally freeze-concentrated fraction [39], known as T'_g. To ensure the total solidification of frozen samples, they should be cooled below their T'_g [31].

The freeze–thawing assay has previously been reported as a simple and fast technique to predict the cryoprotection capacity of pharmaceutical excipients [35]. The complete lyophilization process demands several days, while this assay can be completed over 24 h. In this context, it appears to be a useful preliminary approach to screen the optimal nature and concentration of the cryoprotectant for a specific colloidal system. The premise is that an excipient that cannot protect the micelles during the freezing stage will be unlikely to protect them during lyophilization [44].

With the aim of stabilizing the RIF-loaded PCL(4500) and PCL(3700) flower-like micelles for further *in vitro* and *in vivo* evaluation, cryoprotectants that accomplish cryoprotection by means of two different mechanisms were evaluated in a broad concentration range (table 2) [38,40,45,46]; these copolymers showed an optimal balance between drug encapsulation capacity and physical stability. In addition, three freezing temperatures were tested for all the copolymer/cryoprotectant combinations.

Saccharides such as glucose, maltose and cyclodextrins (e.g. HPβCD) are among the most common cryoprotectants [31]. They can easily vitrify when the freezing is carried out below their T'_g. Carbohydrates perform by decreasing the osmotic pressure of crystallizing water and by generating an amorphous glass phase in which the nanoparticles remain static. This immobilization prevents aggregation or mechanical stress provoked by ice crystals. Also polyethers such as PEG have been widely used as steric stabilizers of proteins and nanoparticles [33]. PEG molecules adsorb on the micellar surface, stabilizing them by a steric hindrance [31,33]. It is worth stressing that saccharides do not perform as steric stabilizers. In addition, a series of saccharide/PEG cryoprotectant mixtures was implemented to explore the benefits of synergistic cryoprotection.

After freeze–thawing, non-cryoprotected micelles showed a dramatic growth to sizes greater than 6 μm (tables 3 and 4). Also, samples were turbid to the naked eye. Considering that the micelles display PEG blocks on the surface, PEG crystallization could take place during the freezing step [31]. Thus, the formation of intra- and inter-particular bridges of crystallized PEG may induce micellar aggregation. For cryoprotected samples that were frozen at −20°C, the thawing was not successful (data not shown), regardless of the cryoprotectant. Samples were completely turbid and the micellar size and size distribution could not be measured by DLS for any of the combinations. When the freezing was performed at −80°C, 1 per cent PCL(4500) micelles cryoprotected with maltose (1 : 20), glucose (1 : 5, 1 : 10 and 1 : 20) and HPβCD (1 : 5, 1 : 10, 1 : 20) remained translucent systems upon thawing (table 3). For example, average D_h values with maltose (1 : 20) at −80°C showed a slight size increase from 130.5 to 194.4 nm (table 3). This represented an f_c value of 1.5 (figure 1*a*). Formulations with glucose (1 : 20) exhibited a sharper size growth (and higher PDI). It is well known that disaccharides such as maltose offer a better cryoprotectant effect than monosaccharides such as glucose [47]. This behaviour is intimately associated with the T'_g of each sugar; the values of maltose and glucose are −29.5°C and −45°C, respectively (table 2). At a certain freezing temperature, the vitreous matrix that prevents micellar aggregation will be more stable for a higher T'_g [45]. Since the freeze–thawing assays were performed below the T'_g of maltose and glucose, the best performance was shown by the disaccharide. Samples with lower

Table 3. Size and size distribution of RIF-loaded PCL(4500) micelles before and after the freeze–thawing assay. Values are expressed as mean ± s.d. ($n = 3$). Aggregation scale: √, no macroscopic aggregation; +++, significant macroscopic aggregation.

			PCL(4500)							
			before freezing		after thawing (−80°C)[b]			after thawing (−196°C)[c]		
copolymer concentration (%w/v)	cryoprotectant	ratio[a]	D_h (nm) (±s.d.)	PDI (±s.d.)	aggregation scale	D_h (nm) (±s.d.)	PDI (±s.d.)	aggregation scale	D_h (nm) (±s.d.)	PDI (±s.d.)
1	no cryoprotectant	—	183.1 (4.7)	0.290 (0.010)	+++	>6 μm	—	+++	>6 μm	—
	maltose	1 : 5	117.7 (24.3)	0.260 (0.094)	+++	>6 μm	—	+++	>6 μm	—
		1 : 10	126.3 (1.1)	0.354 (0.016)	+++	>6 μm	—	+++	>6 μm	—
		1 : 20	130.5 (5.1)	0.187 (0.008)	√	194.4 (40.5)	0.216 (0.019)	√	146.7 (7.7)	0.188 (0.005)
	glucose	1 : 5	102.9 (6.0)	0.197 (0.003)	√	183.0 (6.8)	0.202 (0.008)	+++	>6 μm	—
		1 : 10	114.0 (3.4)	0.199 (0.012)	√	158.4 (11.7)	0.176 (0.030)	√	290.4 (13.4)	0.245 (0.016)
		1 : 20	129.6 (7.6)	0.207 (0.006)	√	234.2 (74.1)	0.263 (0.062)	√	357.9 (142.3)	0.349 (0.102)
	HPβCD	1 : 5	105.7 (5.3)	0.187 (0.006)	√	149.9 (2.4)	0.229 (0.012)	√	134.0 (3.2)	0.211 (0.006)
		1 : 10	134.1 (1.4)	0.189 (0.021)	√	129.6 (14.2)	0.208 (0.005)	√	120.9 (16.6)	0.180 (0.020)
		1 : 20	164.4 (4.8)	0.211 (0.014)	√	177.9 (36.5)	0.227 (0.016)	√	163.7 (28.9)	0.210 (0.015)
	PEG3350	1 : 5	149.2 (3.3)	0.152 (0.011)	+++	>6 μm	—	√	561.9 (17.6)	0.427 (0.045)
	PEG3350/maltose (50/50)	1 : 20	380.6 (21.3)	0.117 (0.042)	√	404.6 (10.1)	0.199 (0.016)	√	319.3 (18.8)	0.205 (0.014)
	PEG3350/glucose (50/50)	1 : 10	190.3 (15.9)	0.175 (0.014)	+++	>6 μm	—	√	195.8 (3.1)	0.167 (0.006)
		1 : 20	258.8 (10.0)	0.142 (0.037)	√	446.0 (77.9)	0.239 (0.008)	√	345.2 (8.8)	0.206 (0.019)
4	no cryoprotectant	—	152.3 (7.8)	0.330 (0.050)	+++	>6 μm	—	+++	>6 μm	—
	HPβCD	1 : 2.5	299.9 (9.2)	0.228 (0.005)	+++	>6 μm	—	√	535.5 (21.6)	0.437 (0.015)
		1 : 5	405.9 (6.4)	0.198 (0.004)	√	572.0 (102.5)	0.370 (0.088)	√	508.4 (35.1)	0.282 (0.012)
6	no cryoprotectant	—	1025.7 (66.6)	0.519 (0.051)	+++	>6 μm	—	+++	>6 μm	—
	HPβCD	1 : 2.5	727.9 (21.0)	0.266 (0.001)	+++	>6 μm	—	√	1355.0 (279.4)	0.495 (0.066)
		1 : 5	994.0 (22.0)	0.212 (0.004)	√	1104.6 (15.1)	0.256 (0.020)	√	1068.7 (26.8)	0.252 (0.010)

[a]Copolymer:cryoprotectant ratio (wt : wt).
[b]Freezing at −80°C.
[c]Freezing by immersion with liquid nitrogen.

Table 4. Size and size distribution of RIF-loaded PCL(3700) micelles before and after the freeze–thawing assay. Values are expressed as mean ± s.d. ($n = 3$). Aggregation scale: √, no macroscopic aggregation; +++, significant macroscopic aggregation.

			PCL(3700)							
			before freezing		after thawing (−80°C)[b]			after thawing (−196°C)[c]		
copolymer concentration (%w/v)	cryoprotectant	weight ratio[a]	D_h (nm) (±s.d.)	PDI (±s.d.)	aggregation scale	D_h (nm) (± s.d.)	PDI (s.d.)	aggregation scale	D_h (nm) (±s.d.)	PDI (s.d.)
1	no cryoprotectant	—	75.4 (11.0)	0.220 (0.010)	+++	>6 µm	—	+++	>6 µm	—
	maltose	1 : 5	86.4 (3.5)	0.192 (0.014)	+++	>6 µm	—	+++	>6 µm	—
		1 : 10	102.6 (15.7)	0.268 (0.096)	+++	>6 µm	—	+++	>6 µm	—
		1 : 20	120.4 (6.5)	0.220 (0.014)	+++	>6 µm	—	√	287.9 (11.3)	0.256 (0.040)
	glucose	1 : 5	87.6 (7.5)	0.231 (0.007)	+++	>6 µm	—	+++	>6 µm	—
		1 : 10	94.1 (3.7)	0.240 (0.061)	√	221.3 (16.6)	0.170 (0.051)	+++	>6 µm	—
		1 : 20	108.4 (14.8)	0.299 (0.058)	√	309.9 (58.1)	0.256 (0.058)	√	320.4 (26.6)	0.330 (0.017)
	HPβCD	1 : 5	87.6 (4.6)	0.192 (0.012)	√	128.3 (9.9)	0.264 (0.039)	√	102.1 (18.6)	0.199 (0.007)
		1 : 10	153.9 (5.4)	0.292 (0.029)	√	112.7 (3.8)	0.235 (0.012)	√	117.7 (11.6)	0.187 (0.014)
		1 : 20	163.3 (4.3)	0.335 (0.009)	√	229.2 (45.2)	0.256 (0.040)	√	147.8 (41.4)	0.200 (0.015)
	PEG3350	1 : 5	127.0 (7.5)	0.157 (0.024)	+++	>6 µm	—	√	416.4 (103.0)	0.337 (0.074)
	PEG3350/maltose (50/50)	1 : 20	236.3 (12.9)	0.239 (0.014)	√	300.3 (8.0)	0.248 (0.004)	√	267.1 (6.5)	0.231 (0.059)
	PEG3350/glucose (50/50)	1 : 10	134.8 (0.9)	0.154 (0.015)	+++	>6 µm	—	√	171.1 (4.2)	0.190 (0.009)
		1 : 20	222.2 (2.0)	0.142 (0.018)	√	380.3 (29.2)	0.244 (0.028)	√	285.8 (20.5)	0.208 (0.009)
4	no cryoprotectant	—	148.3 (12.1)	0.330 (0.030)	+++	>6 µm	—	+++	>6 µm	—
	HPβCD	1 : 2.5	224.0 (8.4)	0.594 (0.085)	√	512.6 (151.1)	0.516 (0.095)	√	421.3 (9.8)	0.257 (0.077)
		1 : 5	261.0 (38.0)	0.604 (0.061)	√	430.7 (82.0)	0.430 (0.040)	√	330.3 (20.0)	0.275 (0.017)
6	No cryoprotectant	—	1041.2 (97.2)	0.549 (0.230)	+++	>6 µm	—	+++	>6 µm	—
	HPβCD	1 : 5	532.0 (25.8)	0.229 (0.005)	√	880.5 (91.2)	0.383 (0.025)	√	758.8 (48.9)	0.346 (0.030)

[a]Copolymer:cryoprotectant ratio (wt : wt).
[b]Freezing at −80°C.
[c]Freezing by immersion with liquid nitrogen.

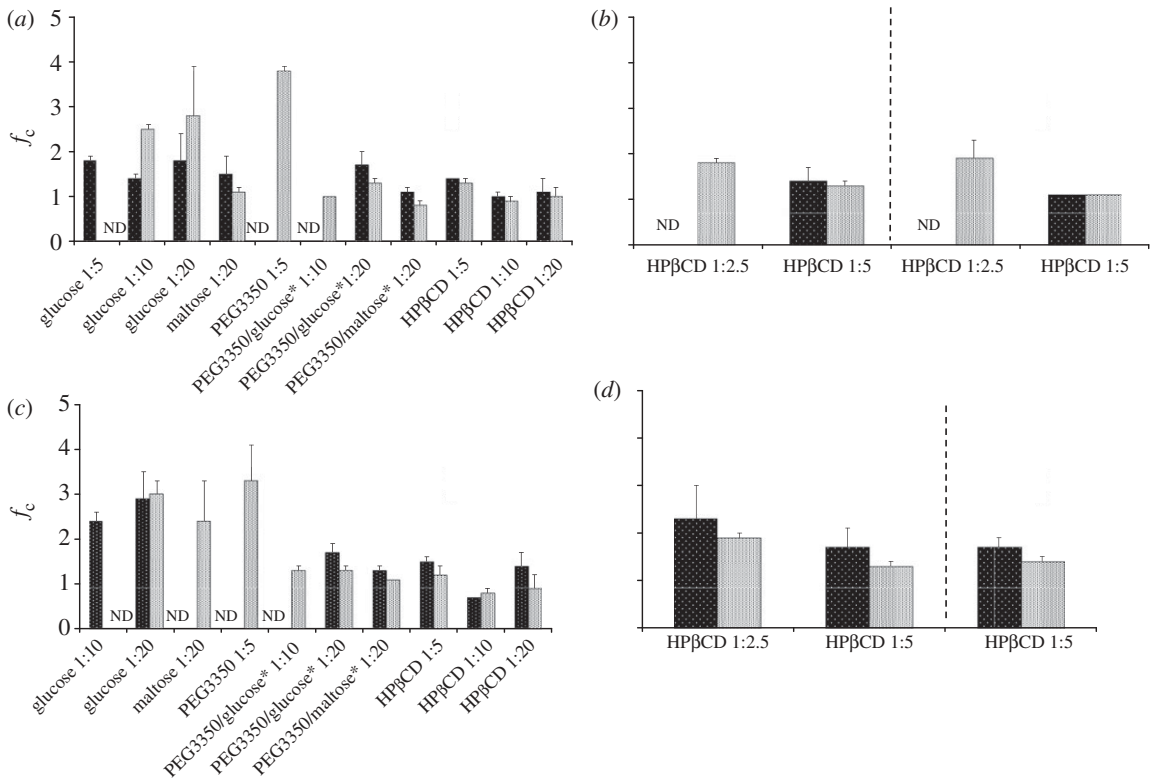

Figure 1. f_c values for (*a*) 1% and (*b*) 4% and 6% RIF-loaded PCL(4500) micelles; (*c*) 1% and (*d*) 4% and 6% RIF-loaded PCL(3700) micelles after the freeze–thawing assay. Cryoprotectants were used in different copolymer:cryoprotectant weight ratios (wt : wt). Samples were frozen at −80°C (black bar with white dots) and −196°C (white bars with black dots). Asterisk, PEG3350/glucose (50 : 50) and PEG3350/maltose (50 : 50). ND, not determined.

ratios of maltose (1 : 5 and 1 : 10) had values of $f_c \gg 2$; the average sizes being greater than 6 μm. These data indicated that a minimal excipient concentration is needed to prevent an excessive micellar size increase [35]. Furthermore, it was found that the stabilization of a cryoprotected system depended on the nanoparticle/cryoprotectant weight ratio and not only on the bulk concentration of the additive [47]. Noticeably, the addition of saccharide cryoprotectants to 1 per cent PCL(4500) led to a clear decrease in the micellar size from 183.1 to 102.2–130.5 nm, even before the freezing stage (table 3). This behaviour suggested that micellar aggregation was already taking place and that, upon addition, sugar molecules were adsorbed on the micellar surface, stabilizing the colloidal system and preventing an irreversible aggregation. Similar observations were reported for PLA nanoparticles [48]. PEG3350 showed the same trend, although to a more limited extent. One per cent PCL(3700) did not display this phenomenon (table 4). The cryoprotection of 1 per cent PCL(3700) by means of saccharides at −80°C was partially effective and only with the greatest glucose concentrations (1 : 10 and 1 : 20) (table 4), the f_c value being 2.4 and 2.9, respectively. With maltose (1 : 20), a greater size increase was observed (table 4). A more rapid freezing rate led to a slight f_c decrease to 2.4, a value still greater than the accepted upper limit previously defined (figure 1*c*). This behaviour would stem from the fusion of the relatively less crystalline and unstable PCL cores of this copolymer as opposed to the counterpart bearing longer PCL blocks. A faster cooling rate did not improve the cryoprotective performance of the mono- and disaccharides under evaluation (tables 3 and 4). Polyols have also been employed in freeze–thawing assays as cryoprotectants [38]. However, sorbitol at different concentrations showed no cryoprotective effect, regardless of the freezing temperature (table 2).

Another cryoprotectant assayed was PEG3350. Despite its possible crystallization during freezing, it has been used as a stabilizer of proteins and as a coating agent of nanoparticles and it might prevent the fusion of micellar hydrophobic cores [33]. It has been reported that the PEG protective effect depends on the chain length and concentration; the greater the molecular weight, the better the cryoprotection properties. In this framework, three different molecular weights and polymer concentrations were tested. PEG3350-added samples (1 : 5) frozen at −80°C were not cryoprotected. A similar trend was followed when PEG6000 and PEG10 000 were used as additives. In general, samples displayed an important size and PDI increase that could not be measured in the DLS. This behaviour could probably rely on the high viscosity of the system that may limit the freezing rate and induce micellar aggregation before a matrix is formed. A higher cooling rate is expected to hasten the formation of small ice crystals and consequently increase the stability of the formulation [34]. PEG3350-added CL(3700) and CL(4500) copolymer micelles (1%) frozen at −196°C were apparently cryoprotected as they appeared completely translucent. However, f_c values were between 3.3 and 3.8, revealing that, in fact, secondary aggregation was not

prevented (figure 1*a,c*). These findings stress the need for a thorough evaluation of the systems.

To explore the benefits of a dual cryoprotection mechanism, maltose/PEG3350 and glucose/PEG3350 mixtures were also assayed. The best results were observed with maltose/PEG3350 combinations (1 : 10 for each excipient, 1 : 20 total) in 1 per cent copolymer systems (figure 1*a,c*). For example, 1 per cent PCL(4500) micellar sizes grew from 380.6 to 404.6 ($f_c = 1.1$) and 319.3 nm ($f_c = 0.8$) at −80°C and −196°C, respectively (figure 1*a*). Similar results were obtained with 1 per cent PCL(3700) (table 4). It is worth stressing that this performance was not attained when maltose was assayed separately at the same concentration (table 3). These results stem from two different additive mechanisms which contribute to the cryoprotective effect and the prevention of the micellar aggregation [49]. When glucose/PEG3350 (1 : 10) mixtures were assessed, stabilization was observed only at −196°C. This behaviour could be attributed to the concentration-dependent cryoprotection. Excipient concentration was not enough to form a uniform matrix around the micelles and protect them from aggregation during the freezing step.

Previous studies have employed these amphiphilic poly(ether–ester) copolymers only in relatively low concentrations, usually below 1–2%. The cryoprotection of more concentrated systems demands the use of highly effective cryoprotectants. Despite the cooling rate employed, none of the mono- and disaccharides, PEG and their combinations prevented the aggregation of the 4 and 6 per cent micelles. In this context, the performance of HPβCD was investigated; these pharmaceutical excipients display the cryoprotection mechanism of other saccharides. This cyclodextrin is an intrinsically amorphous compound that displays high water solubility [50] and a T_g' value of approximately −14°C, a higher value than other saccharides under study (table 2). Low weight ratios (1 : 5) of HPβCD added to both 1 per cent micellar formulations resulted in a minimal size increase. For example, PCL(4500) micelles grew from 105.7 to 149.9 nm (f_c =1.4) (freezing at −80°C) and 134.0 nm (f_c =1.3) (freezing at −196°C) (table 3). A greater excipient concentration (1 : 10) resulted in f_c values of 1.0 and 0.9 (figure 1*a*) for slow and rapid cooling rates, respectively. These results indicate that HPβCD is more effective than mono- and disaccharides, even at lower concentrations [32]. Remarkably, HPβCD (1 : 2.5 and 1 : 5) cryoprotected 4 and 6 per cent micelles (tables 3 and 4). In these cases, size growths similar to those obtained for 1 per cent micelles were apparent. For example, 4 per cent PCL(3700) presented f_c values of 1.7 and 1.3 for slow or rapid freezing rates, respectively (figure 1*d*). Interestingly, PCL(4500) samples showed lower f_c values than CL(3700) for both freezing temperatures and with copolymer concentrations as high as 6 per cent, f_c values being 1.1 (figure 1*b*). The higher the cyclodextrin concentration was, the more efficient the cryoprotection. Furthermore, 6 per cent copolymer samples without any additives showed a larger micellar size (and greater PDI) than the same sample with HPβCD (1 : 5), before freezing. As previously depicted,

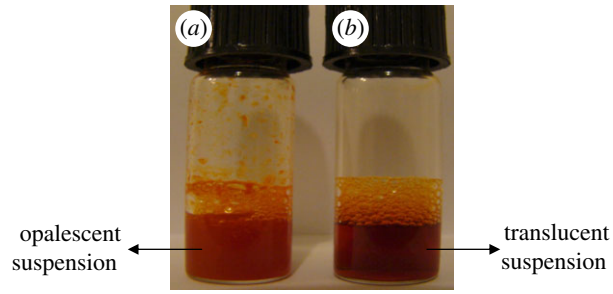

Figure 2. Lyophilized RIF-loaded PCL(4500) micelles (1% w/v) after redispersion in distilled water (*a*) without and (*b*) with the addition of HPβCD (1 : 5). The cryoprotectant effect is given by the complete redispersion of the freeze-dried powder and the translucent appearance of the suspension (*b*). (Online version in colour.)

this may be attributed to the stabilization effect of HPβCD adsorbed on the micellar surface that prevents micellar aggregation (tables 3 and 4). We evaluated the performance of other pristine saccharides such as maltose, glucose and their combinations with PEG3350. However, no cryoprotection was observed.

In advance, only those cryoprotected samples that showed f_c values smaller than 2.0 during the freeze–thawing assays were further evaluated in lyophilization.

3.2. Lyophilization of RIF-loaded micelles

To assess the lyoprotectant capacity of the additives that showed efficient cryoprotection, lyophilization studies were conducted at two freezing temperatures, namely −80°C and −196°C. RIF-loaded PCL–PEG–PCL micelles lyophilized without the addition of excipients were used as controls. After resuspension in distilled water, controls generated opalescent suspensions with average D_h larger than 6 μm (figure 2*a*). This phenomenon stems from the fusion and crystallization of PCL cores of several micelles. When micelles displaying totally amorphous cores (e.g. PEO–PPO) were employed for the encapsulation of antibacterial and antiretroviral agents [51–53], lyophilization/resuspension was possible without the addition of any additive; sizes and size distributions remained unchanged.

Maltose and glucose presented a clear cryoprotectant effect. In addition, they are well known because of their lyoprotectant properties in the freeze-drying of liposomes [39]. Surprisingly, they did not stabilize RIF-loaded PCL–PEG–PCL micelles under the conditions employed in this work. Also, PEG has been reported as an effective lyoprotectant with better protective capacity when it is combined with sugars [39]. Combinations of PEG3350 and maltose or glucose that displayed a cryoprotectant effect in the freeze–thawing assays could not stabilize PCL–PEG–PCL micelles during lyophilization. Only HPβCD at weight ratios of 1 : 5 exhibited a good lyoprotectant effect for RIF-containing micelles with copolymer concentrations between 1 and 6 per cent (tables 5 and 6). For example, 4 and 6 per cent PCL(4500) micelles with HPβCD (1 : 5) showed f_c values less than 1 (figure 3*a*). PCL(3700) systems followed a similar trend, although slightly greater

Table 5. Size and size distribution of RIF-loaded PCL(4500) micelles before and after freeze-drying. Values are expressed as mean ± s.d. ($n = 3$). Aggregation scale: √, no macroscopic aggregation; +++, significant aggregation.

			PCL(4500)							
			before freezing		after lyophilization (−80°C)[b]			after lyophilization (−196°C)[c]		
copolymer concentration (%w/v)	cryoprotectant	weight ratio[a]	D_h (nm) (±s.d.)	PDI (±s.d.)	aggregation scale	D_h (nm) (±s.d.)	PDI (±s.d.)	aggregation scale	D_h (nm) (±s.d.)	PDI (±s.d.)
1	no cryoprotectant	—	183.1 (4.7)	0.290 (0.010)	+++	>6 μm	—	+++	>6 μm	—
	HPβCD	1 : 5	105.7 (5.3)	0.187 (0.006)	√	149.8 (14.3)	0.529 (0.136)	√	114.7 (9.6)	0.199 (0.031)
		1 : 10	134.1 (1.4)	0.189 (0.021)	√	132.0 (8.5)	0.215 (0.007)	√	97.7 (7.1)	0.240 (0.013)
		1 : 20	164.4 (4.8)	0.211 (0.014)	√	144.8 (9.2)	0.243 (0.027)	√	123.4 (6.5)	0.327 (0.027)
4	no cryoprotectant	—	152.3 (7.8)	0.330 (0.050)	+++	>6 μm	—	+++	>6 μm	—
	HPβCD	1 : 5	405.9 (6.4)	0.198 (0.004)	√	356.5 (15.0)	0.404 (0.005)	√	380.5 (31.6)	0.387 (0.018)
6	no cryoprotectant	—	1025.7 (66.6)	0.519 (0.051)	+++	>6 μm	—	+++	>6 μm	—
	HPβCD	1 : 5	994.0 (22.0)	0.212 (0.004)	√	734.3 (126.7)	0.335 (0.095)	√	727.7 (58.7)	0.316 (0.036)

[a]Polymer:cryoprotectant ratio (wt : wt).
[b]Freezing at −80°C.
[c]Freezing by immersion with liquid nitrogen.

Table 6. Size and size distribution of RIF-loaded PCL(3700) micelles before and after freeze-drying. Values are expressed as mean ± s.d. ($n = 3$). Aggregation scale: √, no macroscopic aggregation; +++, significant aggregation.

			PCL(3700)							
			before freezing		after lyophilization (−80°C)[b]			after lyophilization (−196°C)[c]		
copolymer concentration (%w/v)	cryoprotectant	weight ratio[a]	D_h (nm) (±s.d.)	PDI (±s.d.)	aggregation scale	D_h (nm) (±s.d.)	PDI (±s.d.)	aggregation scale	D_h (nm) (±s.d.)	PDI (±s.d.)
1	no cryoprotectant	—	75.4 (11.0)	0.220 (0.010)	+++	>6 μm	—	+++	>6 μm	—
	HPβCD	1 : 5	87.6 (4.6)	0.192 (0.012)	√	147.2 (15.4)	0.444 (0.122)	√	112.1 (18.2)	0.216 (0.036)
		1 : 10	153.9 (5.4)	0.292 (0.029)	√	92.5 (2.5)	0.240 (0.053)	√	106.8 (2.1)	0.224 (0.028)
		1 : 20	163.3 (4.3)	0.335 (0.009)	√	115.5 (7.3)	0.285 (0.057)	√	142.7 (7.6)	0.257 (0.030)
4	no cryoprotectant	—	148.3 (12.1)	0.330 (0.030)	+++	>6 μm	—	+++	>6 μm	—
	HPβCD	1 : 5	261.0 (38.0)	0.604 (0.061)	√	341.1 (12.67)	0.440 (0.030)	√	294.1 (38.7)	0.470 (0.121)
6	no cryoprotectant	—	1041.2 (97.2)	0.549 (0.230)	+++	>6 μm	—	+++	>6 μm	—
	HPβCD	1 : 5	532.0 (25.8)	0.299 (0.005)	√	1048.8 (64.5)	0.448 (0.028)	√	541.1 (100.9)	0.347 (0.085)

[a]Polymer:cryoprotectant ratio (wt : wt).
[b]Freezing at −80°C.
[c]Freezing by immersion with liquid nitrogen.

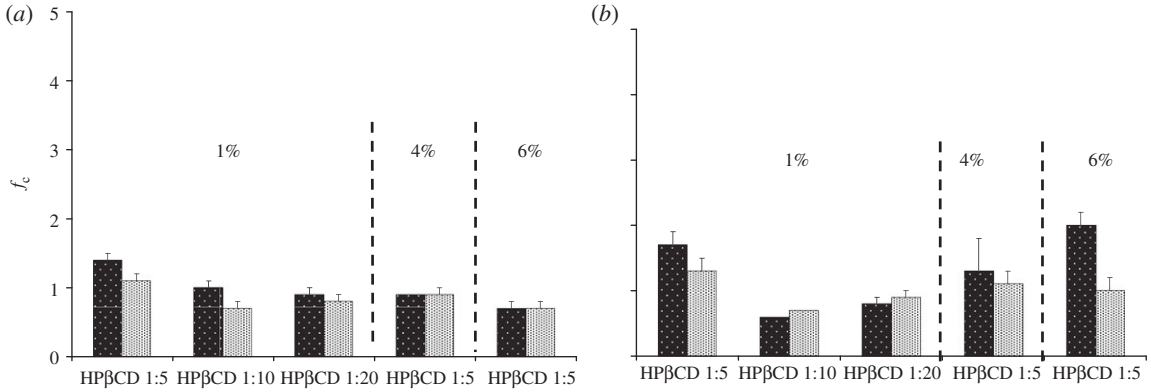

Figure 3. f_c values of RIF-loaded (*a*) PCL(4500) and (*b*) PCL(3700) micelles after the freeze-drying assay. HPβCD was used in different copolymer:cryoprotectant weight ratios (wt : wt). Samples were frozen at −80°C (black bar with white dots) and −196°C (white bar with black dots).

Table 7. Zeta potential values of RIF-loaded PCL(3700) and PCL(4500) micelles before and after lyophilization. Values are expressed as mean ± s.d. ($n = 3$).

		zeta potential (mV) (±s.d.)			
		PCL(3700)		PCL(4500)	
copolymer concentration (%w/v)	ratio[a]	before lyophilization	after lyophilization	before lyophilization	after lyophilization
1	1 : 5	−1.17 (0.17)	+1.74 (0.31)	−1.04 (0.14)	+1.52 (0.08)
	1 : 10	−0.96 (0.28)	+0.50 (0.02)	−0.93 (0.01)	+1.31 (0.02)
	1 : 20	−1.26 (0.16)	−0.42 (0.10)	−0.87 (0.07)	+1.00 (0.04)
4	1 : 5	+0.22 (0.02)	+0.70 (0.05)	−0.09 (0.09)	+0.52 (0.08)
6	1 : 5	−0.18 (0.02)	+0.20 (0.04)	−0.62 (0.10)	+0.26 (0.03)

[a]Copolymer:cryoprotectant (wt : wt).

PDI values were observed (table 6). These data indicated that, regardless of successful lyoprotection, some level of micellar secondary aggregation was taking place at relatively low HPβCD concentrations; a very small size population of larger size was apparent also in DLS analysis.

The lyophilisates presented a uniform aspect and their dry volume was identical to that of the initial colloidal suspension. Also, freeze-dried samples could be redispersed easily in distilled water. This behaviour indicated the absence of powder collapse [54]. After redispersion, systems remained translucent without any visible aggregates (figure 2*b*).

Zeta potential measurements of the cryoprotected micellar systems before and after lyophilization showed no relevant changes (table 7). Before freeze-drying, the systems presented values between −1.26 and +0.22 mV. After lyophilization, values were between −0.42 and +1.74 mV. These data were in agreement with previous work, in which the surface of RIF-free and RIF-loaded PCL–PEG–PCL micelles was analysed [25]. DLS measurements revealed f_c values usually smaller than 1.5 for both freezing temperatures, except PCL(3700) frozen at −80°C ($f_c = 1.7$ and 2) (figure 3*a,b*). This deleterious effect is probably related to the slow freezing temperature that hastens the ability of shorter and less crystalline PCL cores to agglomerate and fuse. Moreover, some resuspended samples showed $f_c < 1$, this phenomenon being attributed to a micellar contraction during the freeze-drying process. Overall these data suggest a successful lyophilization process.

It has been reported that a successful lyophilization cycle is governed by (i) the thermal properties (T_g') of the cryoprotectant/lyoprotectant and (ii) the conservation of its collapse temperature (T_c) [55]; T_c is defined as the maximum allowable temperature for primary drying. In general, the difference between T_g' and T_c is approximately 1–2°C [54,55]. Since products can collapse when they are heated above the T_g'/T_c (during the sublimation step) [40], it is desirable that the addition of the nanoparticles does not modify substantially these thermal parameters. Thus, two conditions apply for a successful lyophilization: (i) the freezing step should be conducted at a temperature at least 10°C lower than the T_g' of the lyoprotectant carbohydrate and (ii) the primary drying temperature should be set 5–10°C below the T_g'/T_c to obtain porous lyophilized cakes [39]. Considering the conditions used in this work, freezing was carried out below the T_g' of every additive or mixture. Therefore, a glassy matrix was primarily formed. However, primary drying was carried out at −14°C (shelf temperature). This temperature was higher than the T_g' of maltose and glucose (table 2) and may account for the collapse of samples lyoprotected with these sugars; the porous matrix structure formed by the lyoprotectant was lost after ice sublimation.

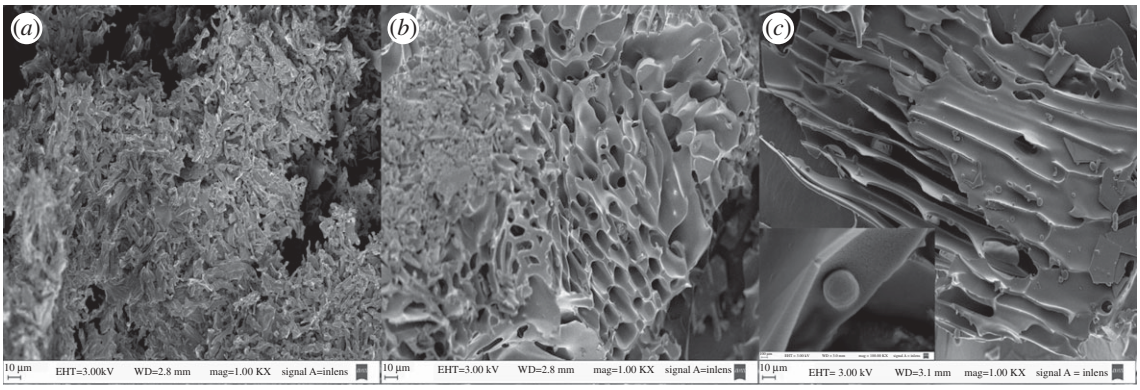

Figure 4. SEM microphotographs of freeze-dried samples of (*a*) 1% RIF-loaded PCL(4500) micelles without cryoprotection (control), (*b*) freeze-dried 5% HPβCD solution (control) and (*c*) 1% RIF-loaded PCL(4500) micelles containing HPβCD (1 : 5 copolymer:cryoprotectant weight ratio). Scale bar, 10 µm. Photo inset: magnification of (*c*); scale bar, 100 nm. All the samples were frozen by immersion in liquid nitrogen (−196°C), prior to lyophilization.

For sugar/PEG3350 combinations, the T_g' estimated values presented in table 2 were far below −14°C. Thus, regardless of the combined lyoprotective mechanism, samples underwent significant aggregation. When HPβCD was used, no collapse was observed, this phenomenon being irrespective of the freezing temperature applied. This is probably associated with the relatively high T_g' of HPβCD (table 2). It is worth mentioning that the experimental value determined by DSC (−13.9 ± 2°C) was in the range of the one reported in the literature [40]. Even though the primary drying was not conducted 5°C below the T_g' of the cryoprotectant, it seems that it maintained its stabilizing effect and the lyophilisate could be redispersed with a minor micellar size increase. These results are in agreement with previous studies that investigated the freeze-drying of PCL nanocapsules [55].

To assess the chemical stability of RIF upon the lyophilization, the drug concentration was determined by UV, as previously described in §2.3. RIF payloads remained unchanged. In addition, the random analysis of samples by HPLC indicated the presence of one single elution fraction that corresponded to RIF.

3.3. Morphological characterization of freeze-dried RIF-loaded micelles

The microstructure of lyophilized RIF-loaded 1 per cent PCL–PEG–PCL micelles freeze-dried with 1 : 5 HPβCD was visualized by FEG-SEM and AFM. RIF-loaded 1 per cent PCL(4500) micelles freeze-dried without any lyoprotectant and lyophilized with 5 per cent HPβCD were used as controls. When the micelles were lyophilized without stabilization, the sample showed large irregular aggregates (figure 4*a*). This structure has been recently reported for poly(ϵ-caprolactone–co-4-maleate–ϵ-caprolactone) nanoparticles [56]. In addition, the absence of singular micelles was consistent with DLS measurements. With HPβCD, a porous amorphous matrix, which hosted spherical RIF-loaded micelles, was formed (figure 4*c*). The micellar size calculated by FEG-SEM was greater than the average D_h obtained by DLS and more than one population was observed. SEM gives precise morphological information, although the preparation method included Au shadowing of the sample (film coating). The gold layer obtained may alter the average diameter of the micelles, leading to an increase in the micellar size. Considering this, SEM and DLS data were in good agreement. For comparison, the SEM microphotograph of freeze-dried 5 per cent HPβCD shows an amorphous matrix without the presence of spherical micelles (figure 4*b*).

To gain further insight into the morphology of the cryoprotected RIF-loaded micelles, but in an aqueous environment, we conducted tapping mode AFM analysis. Specimens (1%) were conveniently diluted before the analysis (1 : 20). The presence of spherical micelles (diameter = 87–116 nm) is shown in figure 5*b*,*c*. The smaller height (12–29 nm) of the micelles with respect to their diameter revealed that they were embedded in the cryoprotectant matrix. In addition, the micellar size determined by AFM was consistent with data obtained by DLS (105.7 and 114.7 nm before and after lyophilization, respectively). Interestingly, RIF-loaded PCL micelles that were analysed by AFM immediately after their preparation and addition of cryoprotectant did not present the spherical structures shown by their lyophilized counterparts (figure 5*a*). This phenomenon is related to the fact that, after water sublimation, the PCL cores of the micelles exposed to lyophilization crystallize to a greater extent, making micelles more stable under dilution. In the case of non-lyophilized samples this stabilization was less feasible.

3.4. Thermal properties upon lyophilization

DSC analysis of freeze-dried RIF-free and RIF-loaded PCL–PEG–PCL micelles at different copolymer concentrations was carried out to establish possible interactions between the drug, the copolymer and the cryoprotectant (HPβCD). Based on the previous assays, combinations of copolymer:cryoprotectant (1 : 5) provided good lyoprotection, regardless of the copolymer concentration. Therefore, this study focused on combinations of 1 and 6 per cent copolymer micelles and HPβCD. DSC of lyophilized HPβCD and pristine and lyophilized RIF were used as controls (table 8).

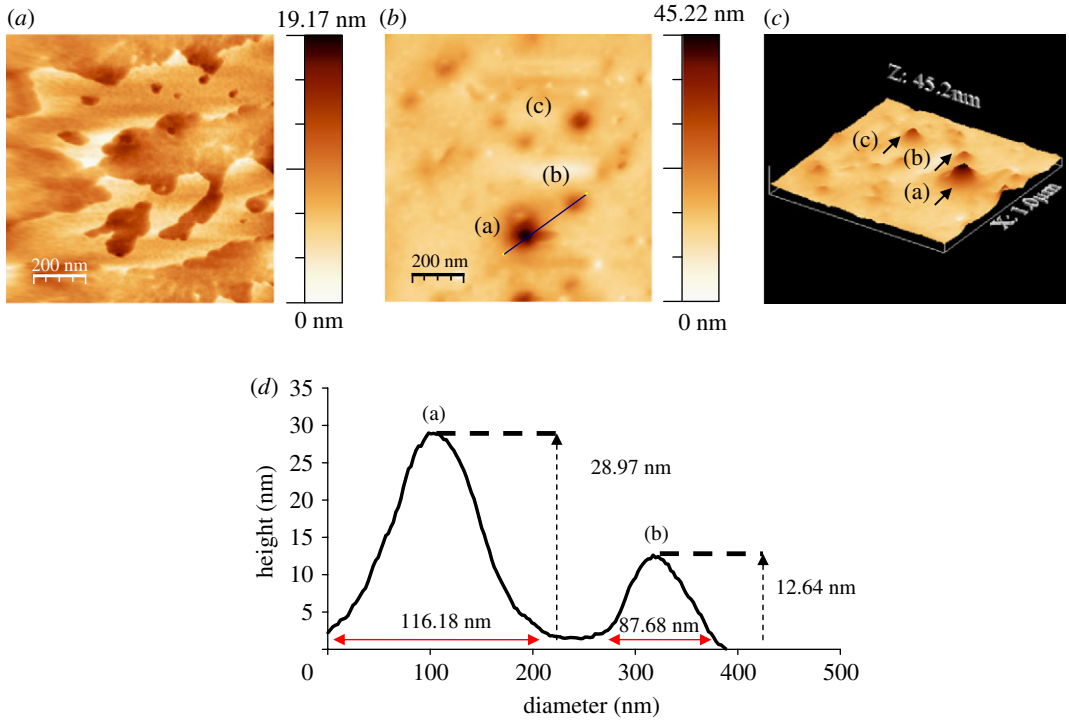

Figure 5. Tapping mode AFM phase two-dimensional images of (*a*) fresh and (*b*) freeze-dried 1% w/v RIF-loaded PCL(4500) micelles cryoprotected with HPβCD 1 : 5 (copolymer:cryoprotectant weight ratio) and diluted (1 : 20) immediately before the analysis. (*c*) Same as (*b*) but three dimensional. (*d*) AFM height versus diameter profile of the structures (a and b) pointed out in (*b*,*c*). The micelle pointed out in (*b*,*c*) as (c) presents a height of 17.18 nm and diameter of 68.84 nm. (Online version in colour.)

Table 8. DSC analysis of non-lyophilized and lyophilized RIF-loaded micelles containing 1% and 6% copolymer. Pristine and lyophilized RIF, lyophilized RIF-free micelles and lyophilized cryoprotectant (HPβCD) were used as control. S2–S13 were freeze-dried (freezing was conducted by immersion in liquid nitrogen). S4,S5,S8,S9,S10,S11, original copolymer concentration was 1%. S6,S7,S12,S13, original copolymer concentration was 6% w/v.

		sample composition (%)				copolymer PCL–PEG–PCL		HPβCD		RIF
	sample	copolymer PCL(3700)	copolymer PCL(4500)	HPβCD	RIF	T_m (°C)	ΔH_m (J g^{-1})	T_{deh} (°C)	T_{decomp} (°C)	T_{decomp} (°C)
pristine RIF	S1	—	—	—	100	—	—	—	—	253.8
lyophilized RIF	S2	—	—	—	100	—	—	—	—	171.2/ 253.6
HPβCD	S3	—	—	100	—	—	—	104.8	266.0	—
PCL–PEG–PCL	S4	—	100	—	—	52.2	93.2	—	—	—
unloaded	S5	100	—	—	—	50.4	87.3	—	—	—
micelles	S6	—	100	—	—	52.6	90.1	—	—	—
	S7	100	—	—	—	51.4	99.7	—	—	—
binary systems[a]	S8	—	67.5	—	32.5	49.5	93.6	—	—	244.0
	S9	67.8	—	—	32.2	50.4	127.1	—	—	245.7
ternary systems[b]	S10	—	15.4	77.4	7.2	46.1	7.5	104.3	—	249.1
	S11	15.4	—	77.3	7.3	45.6	7.4	101.8	—	254.2
	S12	—	16.1	80.8	3.1	47.8	13.3	100.2	—	258.6
	S13	16.2	—	80.7	3.1	39.6	12.6	109.9	—	259.0

[a]Binary system: RIF-loaded PCL–PEG–PCL micelles.
[b]Ternary system: RIF-loaded PCL–PEG–PCL micelles cryoprotected with HPβCD. Copolymer: HPβCD weight ratio (1 : 5).

Pristine RIF showed the thermal behaviour of polymorphic form I [57], in which the only thermal transition observed is a single decomposition exotherm. After lyophilization the thermal properties of the pure drug were altered. The presence of two decomposition exotherms suggests its conversion into the amorphous form (table 8) [58], while the broad endothermic peak between 40°C and 110°C could be attributed to residual lyophilization water. The amorphous HPβCD displayed only a broad endothermic peak between 50°C and 120°C, which is characteristic of the loss of free and bounded water (table 8). RIF-free PCL–PEG–PCL micelles

Table 9. Residual water in different HPβCD-lyoprotected RIF-loaded micelles upon lyophilization as determined by the Karl Fisher method ($n = 3$).

sample	copolymer concentration (%w/v)	water content (%wt) (±s.d.)
PCL(3700)	1	2.95 (0.49)
	4	0.89 (0.01)
	6	1.11 (0.23)
PCL(4500)	1	2.90 (0.26)
	4	0.81 (0.02)
	6	1.20 (0.26)

showed only one endothermic peak that corresponded to the melting of both PEG and PCL in the copolymer. Lyophilized RIF-loaded micelles deprived of cryoprotectant displayed one endothermic peak at 49.5°C ($\Delta H_m = 93.6\ J\ g^{-1}$) that belongs to the melting of PEG and PCL blocks and one decomposition exotherm of RIF at 244.0°C (table 8). These results suggest that the encapsulation of RIF into the micelles favours the formation of form I RIF. On the other hand, the T_m of the copolymer in RIF-loaded micelles was lower than that of the drug-free system (without a significant decrease in ΔH_m), suggesting the formation of less perfect crystals (table 8). Moreover, the encapsulation of the drug resulted in a reduction in the T_{decomp} when compared with free RIF (table 8). This behaviour probably stemmed from the drug dispersion at the molecular level in the copolymer matrix and a greater sensitivity to heating. When HPβCD was added, T_m and ΔH_m decreased to 46.1°C and 7.5 J g^{-1}, respectively. These results indicate a strong copolymer/HPβCD interaction, the cryoprotectant hindering the copolymer crystallization process [59,60].

3.5. Determination of residual water

Residual water is a key stability parameter of freeze-dried formulations. High residual water content is a common consequence of the collapse of the product over the lyophilization [54]. In addition, the thermal properties of the freeze-dried samples can be modified by residual water. Also, some reports suggested that residual water may cause a reduction in the melting temperature, thus reducing the protective effect according to the vitrification mechanism [39]. Also, water could hydrolyse water-labile drugs [34] such as RIF [18]. Finally, remaining water can promote biological contamination of the product, which leads to insufficient long-term stability. Karl Fisher titration of RIF-loaded micelles with different type and concentration of cryoprotectants at different copolymer concentrations (1–6%) showed that all the samples retained very low residual water of between 0.8 and 3 per cent (table 9). Values were irrespective of the copolymer. These data strongly suggest that the chemical stability of RIF will be fully ensured.

3.6. Physico-chemical stability of lyophilized samples

To evaluate the physical stability of lyoprotected systems, samples were stored in the dry state over one month, at −20°C and 25°C. Then, the size and size distribution of freeze-dried RIF-loaded micelles were measured by DLS and $f'_{c-20°C}$ and $f'_{c25°C}$ values were determined, immediately after reconstitution. All the samples were easily redispersable and remained translucent to the naked eye. $f'_{c-20°C}$ values ranged between 1 and 1.6, while $f'_{c25°C}$ values ranged between 0.9 and 1.9. Considering that the upper limit defined for f_c was 2.0, these results indicated that the samples were stable under these storage conditions. Furthermore, RIF payloads remained completely unchanged, as established by HPLC.

4. CONCLUSIONS

This work demonstrated the feasibility of the successful lyophilization of RIF-loaded PCL–PEG–PCL micelles with an acceptable particle size after reconstitution. The use of cryo/lyoprotective additives has been demonstrated to be essential in order to avoid micellar aggregation. The freeze–thawing studies allowed the screening of the cryoprotection ability of different additives towards the freeze-drying assays. HPβCD at a relatively low weight ratio (1 : 5) has demonstrated the best lyoprotectant effect, enabling for the first time the successful lyoprotection/lyophilization of drug-loaded PCL–PEG–PCL micellar systems of concentrations as high as 6 per cent. Further studies would be necessary to establish the mid- to long-term physico-chemical stability of the freeze-dried systems.

M.A.M. received a PhD scholarship from the CONICET. D.A.C. and A.S. are staff members of the CONICET.

REFERENCES

1 Kaufmann, S. H. & McMichael, A. J. 2005 Annulling a dangerous liaison: vaccination strategies against AIDS and tuberculosis. *Nat. Med.* **11**, S33. (doi:10.1038/nm1221)
2 Frieden, T. R., Sterling, T. R., Munsiff, S. S., Watt, C. J. & Dye, C. 2003 Tuberculosis. *Lancet* **362**, 887. (doi:10.1016/S0140-6736(03)14333-4)
3 Ginsberg, A. M. 2010 Drugs in development for tuberculosis. *Drugs* **70**, 2201. (doi:10.2165/11538170-000000000-00000)
4 Sharma, M. & Thapaliya, H. P. 2009 Tuberculosis—the disease of poverty. *St Xavier's J. Sci.* **1**, 1–9.
5 Jain, S. K., Lamichhane, G., Nimmagadda, S., Pomper, M. G. & Bishai, W. R. 2008 Antibiotic treatment of tuberculosis: old problems, new solutions. *Microbe* **3**, 285–292.
6 WHO. 2008 *Global tuberculosis control 2008: surveillance, planning, financing.* Geneva, Switzerland: World Health Organization. See http://www.who.int/tb/publications/global_report/2008/pdf/fullreport.pdf
7 WHO 1993 WHO declares tuberculosis a global emergency. *Soc. Prevent. Med.* **38**, 251. (doi:10.1007/BF01624546)
8 Onyebujoh, P., Zumla, A., Ribeiro, I., Rustomjee, R., Mwaba, P., Gomes, M. & Grange, J. M. 2005 Treatment of tuberculosis: present status and future prospects. *Bull. World Health Organ.* **83**, 857. (doi:10.1590/S0042-96862005001100016)
9 WHO. 2010 *Treatment of tuberculosis: guidelines*, 4th edn. Geneva, Switzerland: World Health Organization. See http://whqlibdoc.who.int/publications/2010/9789241547833_eng.pdf

10 Brewer, T. & Heymann, S. 2005 Long time due: reducing tuberculosis mortality in the 21st century. *Arch. Med. Res.* **36**, 617–621. (doi:10.1016/j.arcmed.2005.06.002)
11 Dye, C. 2006 Global epidemiology of tuberculosis. *Lancet* **367**, 938–940. (doi:10.1016/S0140-6736(06)68384-0)
12 Rivers, E. C. & Mancera, R. L. 2008 New antituberculosis drugs in clinical trials with novel mechanism of action. *Drug Discov. Today* **13**, 1090–1098. (doi:10.1016/j.drudis.2008.09.004)
13 Becker, C., Dressman, J. B., Junginger, H. E., Kopp, S., Midha, K. K., Shah, V. P., Stavchansky, S. & Barends, D. M. 2009 Biowaiver monographs for immediate release solid oral dosage forms: rifampicin. *J. Pharm. Sci.* **98**, 2252–2267. (doi:10.1002/jps.21624)
14 Zaru, M., Mourtas, S., Klepetsanis, P., Fadda, A. M. & Antimisiaris, S. G. 2007 Liposomes for drug delivery to the lungs by nebulization. *Eur. J. Pharm. Biopharm.* **67**, 655–666. (doi:10.1016/j.ejpb.2007.04.005)
15 Agrawal, S. & Panchagnula, R. 2004 Dissolution test as a surrogate for quality evaluation of rifampicin containing fixed dose combination formulations. *Int. J. Pharm.* **287**, 97–112. (doi:10.1016/j.ijpharm.2004.09.005)
16 Mariappan, T. T. & Singh, S. 2003 Regional gastrointestinal permeability of rifampicin and isoniazid (alone and their combination) in the rat. *Int. J. Tuberc. Lung Dis.* **7**, 797–803.
17 Mariappan, T. T. & Singh, S. 2006 Positioning of rifampicin in the biopharmaceutics classification system (BCS). *Clinical Res. Reg. Affairs* **23**, 1. (doi:10.1080/10601330500533990)
18 Shishoo, C. J., Shah, S. A., Rathod, I. S., Savale, S. S., Kotecha, J. S. & Shah, P. B. 1999 Stability of rifampicin in dissolution medium in presence of isoniazid. *Int. J. Pharm.* **190**, 109–123. (doi:10.1016/S0378-5173(99)00286-0)
19 Singh, S., Mariappan, T. T., Sharda, N., Kumar, S. & Chakrabarti, A. K. 2000 The reason for an increase in decomposition of rifampicin in the presence of isoniazid under acid conditions. *Pharm. Pharmacol. Commun.* **6**, 405–410. (doi:10.1211/146080800128736277)
20 Shishoo, C. J., Shah, S. A., Rathod, I. S., Savale, S. S. & Vora, M. J. 2001 Impaired bioavailability of rifampicin in presence of isoniazid from fixed-dose combination (FDC) formulation. *Int. J. Pharm.* **228**, 53–67. (doi:10.1016/S0378-5173(01)00831-6)
21 Gohel, M. C. & Sarvaiya, K. G. 2007 A novel solid dosage form of rifampicin and isoniazid with improved functionality. *AAPS Pharm. Sci. Tech.* **8**, Article 68. (doi:10.1208/pt0803068)
22 Sosnik, A. & Amiji, M. 2010 Nanotechnology solutions for infectious diseases in developing nations. *Adv. Drug Deliv. Rev.* **62**, 375–377. (doi:10.1016/j.addr.2009.11.010)
23 Sosnik, A., Carcaboso, A. M., Glisoni, R. J., Moretton, M. A. & Chiappetta, D. A. 2010 New old challenges in tuberculosis: potentially effective nanotechnologies in drug delivery. *Adv. Drug Del. Rev.* **62**, 547–559. (doi:10.1016/j.addr.2009.11.023)
24 Griffiths, G., Nyström, B., Sable, S. B. & Khuller, G. K. 2010 Nanobead-based interventions for the treatment and prevention of tuberculosis. *Nat. Rev. Microbiol.* **8**, 827–834. (doi:10.1038/nrmicro2437)
25 Moretton, M. A., Glisoni, R. J., Chiappetta, D. A. & Sosnik, A. 2010 Molecular implications in the nanoencapsulation of the antituberculosis drug rifampicin within flower-like polymeric micelles. *Colloids Surf. B-Biointerfaces* **79**, 467–479. (doi:10.1016/j.colsurfb.2010.05.016)
26 Chiappetta, D. A. & Sosnik, A. 2007 Poly(ethylene oxide)–poly(propylene oxide) block copolymer micelles as drug delivery agents: improved hydrosolubility, stability and bioavailability of drugs. *Eur. J. Pharm. Biopharm.* **66**, 303–317. (doi:10.1016/j.ejpb.2007.03.022)
27 Moretton, M. A., Glisoni, R. J., Chiappetta, D. A., Sosnik, A. & BIOOMAT 2009 Tissue engineering and artificial organs (SLABO). In *Workshop on artificial organs, biomaterials and tissue engineering*. Rosario, Argentina: Latin American Society of Biomaterials.
28 Mehta, S. K., Bhasin, K. K., Mehta, N. & Dham, S. 2005 Behavior of rifampicin in association with β-cyclodextrin in aqueous media: a spectroscopic and conductometric study. *Colloid Polym. Sci.* **283**, 532–538. (doi:10.1007/s00396-004-1181-5)
29 Vijayaraj Kumar, P., Asthana, A., Dutta, T. & Jain, N. K. 2006 Intracellular macrophage uptake of rifampicin loaded mannosylated dendrimers. *J. Drug Target* **14**, 546–556. (doi:10.1080/10611860600825159)
30 Hu, Y., Ding, Y., Li, Y., Jiang, X., Yang, C. & Yang, Y. 2006 Physical stability and lyophilization of poly(ϵ-caprolactone)–*b*-poly(ethyleneglycol)–*b*-poly(ϵ-caprolactone) micelles. *J. Nanosci. Nanotechnol.* **6**, 3032–3039. (doi:10.1166/jnn.2006.432)
31 Abdelwahed, W., Degobert, G., Stainmesse, S. & Fessi, H. 2006 Freeze-drying of nanoparticles: formulation, process and storage considerations. *Adv. Drug Del. Rev.* **58**, 1688–1713. (doi:10.1016/j.addr.2006.09.017)
32 Richter, A., Olbrich, C., Krause, M., Hoffmann, J. & Kissel, T. 2010 Polymeric micelles for parenteral delivery of Sagopilone: physicochemical characterization, novel formulation approaches and their toxicity assessment *in vitro* as well as *in vivo*. *Eur. J Pharm. Biopharm.* **75**, 80. (doi:10.1016/j.ejpb.2010.02.010)
33 Yang, Z. L., Li, X. R., Yang, K. W. & Liu, Y. 2008 Amphotericin B-loaded poly(ethylene glycol)-poly(lactide) micelles: preparation, freeze drying and *in vitro* release. *J. Biomed. Mat. Res. Part A.* **85A**, 539–546. (doi:10.1002/jbm.a.31504)
34 Di Tommaso, C., Como, C., Gurny, R. & Möller, M. 2010 Investigations on the lyophilisation of MPEG–hexPLA micelle based pharmaceutical formulations. *Eur. J. Pharmacol. Sci.* **40**, 38–47. (doi:10.1016/j.ejps.2010.02.006)
35 Date, P. V., Samad, A. & Devarajan, P. V. 2010 Freeze thaw: a simple approach for prediction of optimal cryoprotectant for freeze drying. *AAPS Pharm. Sci. Tech.* **11**, 304–313. (doi:10.1208/s12249-010-9382-3)
36 Gotelli, G., Bonelli, P., Abraham, G. & Sosnik, A. 2011 Fast and efficient synthesis of high molecular weight poly(ϵ-caprolactone) diols by microwave-assisted polymer synthesis (MAPS). *J. Appl. Polym. Sci.* **121**, 1321–1329. (doi:10.1016/j.progpolymsci.2010.12.001)
37 Sosnik, A., Gotelli, G. & Abraham, G. A. 2011 Microwave-assisted polymer synthesis (MAPS) as a tool in biomaterials science: how new and how powerful. *Prog. Polym. Sci.* **36**, 1050–1078. (doi:10.1016/j.progpolymsci.2010.12.001)
38 Saez, A., Guzmán, M., Molpeceres, J. & Aberturas, M. R. 2000 Freeze-drying of polycaprolactone and poly (D,L-lactic-glycolic) nanoparticles induce minor particle size changes affecting the oral pharmacokinetics of loaded drugs. *Eur. J. Pharm. Biopharm.* **50**, 379–387. (doi:10.1016/S0939-6411(00)00125-9)
39 Chen, C., Han, D., Cai, C. & Tang, X. 2010 An overview of liposome lyophilization and its future potential. *J. Controll. Rel.* **142**, 299–311. (doi:10.1016/j.jconrel.2009.10.024)
40 Abdelwahed, W., Degobert, G. & Fessi, H. 2006 Investigation of nanocapsules stabilization by amorphous excipients during freeze-drying and storage. *Eur.*

J. Pharm. Biopharm. **63**, 87–94. (doi:10.1016/j.ejpb.2006.01.015)

41 Holzer, M., Vogel, V., Mäntele, W., Schwartz, D., Haase, W. & Langer, K. 2009 Physico-chemical characterisation of PLGA nanoparticles after freeze-drying and storage. *Eur. J. Pharm. Biopharm.* **72**, 428–437. (doi:10.1016/j.ejpb.2009.02.002)

42 Horcas, I., Fernandez, R., Gomez-Rodriguez, J. M., Colchero, J., Gomez-Herrero, J. & Baro, A. M. 2007 WSXM: a software for scanning probe microscopy and a tool for nanotechnology. *Rev. Sci. Instrum.* **78**, 013705. (doi:10.1063/1.2432410)

43 Tang, X. C. & Pikal, M. J. 2004 Design of freeze-drying process for pharmaceuticals practical advice. *Pharm. Res.* **21**, 191–200. (doi:10.1023/B:PHAM.0000016234.73023.75)

44 Schwarz, C. & Mehnert, W. 1997 Freeze-drying of drug-free and drug-loaded solid lipid nanoparticles (SLN). *Int. J. Pharm.* **157**, 171–179. (doi:10.1016/S0378-5173(97)00222-6)

45 Miyajima, K. 1997 Role of saccharides for the freeze–thawing and freeze drying of liposome. *Adv. Drug Del. Rev.* **24**, 151–159. (doi:10.1016/S0169-409X(96)00454-1)

46 Heller, M. C., Carpenter, J. F. & Randolph, T. W. 1999 Aplication of a thermodynamic model to the prediction of phase separations in freeze-concentrated formulations for protein lyophilization. *Arch. Biochem. Biophys.* **363**, 191–201. (doi:10.1006/abbi.1998.1078)

47 Wang, W. 2000 Lyophilization and development of solid protein pharmaceuticals. *Int. J. Pharm.* **203**, 1–2. (doi:10.1016/S0378-5173(00)00423-3)

48 Musumeci, T., Vicari, L., Ventura, C. A., Gulisano, M., Pignatello, R. & Puglisi, G. 2006 Lyoprotected nanosphere formulations for paclitaxel controlled delivery. *J. Nanosci. Nanotech.* **6**, 3118–3125. (doi:10.1166/jnn.2006.452)

49 Layre, A. M., Couvreur, P., Richard, J., Requier, D., Eddine Ghermani, N. & Gref, R. 2006 Freeze-drying of composite core-shell nanoparticles. *Drug Dev. Ind. Pharm.* **32**, 839–846. (doi:10.1080/03639040600685134)

50 Ressing, M. E., Jiskoot, W., Talsma, H., van Ingen, C. W., Coen Beuvery, E. & Crommelin, D. J. A. 1992 The influence of sucrose, dextran and hydroxypropyl-β-cyclodextrin as lyoprotectants for a freeze-dried mouse IgG_{2a} monoclonal antibody (MN12). *Pharm. Res.* **9**, 266–270. (doi:10.1023/A:1018905927544)

51 Chiappetta, D. A., Degrossi, J., Teves, S., D'Aquino, M., Bregni, C. & Sosnik, A. 2008 Triclosan-loaded poloxamine micelles for enhanced antibacterial activity against biofilm. *Eur. J. Pharm. Biopharm.* **69**, 535–545. (doi:10.1016/j.ejpb.2007.03.022)

52 Chiappetta, D. A., Hocht, C., Taira, C. & Sosnik, A. 2010 Efavirenz-loaded polymeric micelles for pediatric anti-HIV pharmacotherapy with significantly higher oral bioavailability. *Nanomedicine* **5**, 11–23. (doi:10.1016/j.ejpb.2007.03.022)

53 Chiappetta, D. A., Hocht, C., Taira, C. & Sosnik, A. 2011 Oral pharmacokinetics of efavirenz-loaded polymeric micelles. *Biomaterials* **32**, 2379. (doi:10.1016/j.ejpb.2007.03.022)

54 Pikal, M. J. & Shah, S. 1990 The collapse temperature in freeze-drying: dependence on measurement methodology and rate of water removal from the glassy phase. *Int. J. Pharm.* **62**, 165–186. (doi:10.1016/0378-5173(90)90231-R)

55 Abdelwahed, W., Degobert, G. & Fessi, H. 2006 A pilot study of freeze-drying of poly(ϵ-caprolactone) nanocapsules stabilized by poly(vinyl alcohol): formulation and process optimization. *Int. J. Pharm.* **309**, 178–188. (doi:10.1016/j.ijpharm.2005.10.003)

56 Zhang, Y., Li, J., Lang, M., Tang, X., Li, L. & Shen, X. 2011 Folate-functionalized nanoparticles for controlled 5-fluorouracil delivery. *J. Colloids Interface Sci.* **354**, 202–209. (doi:10.1016/j.jcis.2010.10.054)

57 Agrawal, S., Ashokraj, Y., Bharatam, P. V., Pillai, O. & Panchagnula, R. 2004 Solid-state characterization of rifampicin samples and its biopharmaceutic relevance. *Eur. J. Pharm. Sci.* **22**, 127–144. (doi:10.1016/j.ejps.2004.02.011)

58 Panchagnula, R. & Bhardwaj, V. 2008 Effect of amorphous content on dissolution characteristics of rifampicin. *Drug Dev. Ind. Pharm.* **34**, 642–649. (doi:10.1080/03639040701842451)

59 Ambrus, R., Aigner, Z., Catenacci, L., Bettinetti, G., Szabó-Révész, P. & Sorrenti, M. 2010 Physico-chemical characterization and dissolution properties of nifluminic acid-cyclodextrin-PVP ternary systems. *J. Therm. Anal. Calorim.* **104**, 291–297. (doi:10.1007/s10973-010-1069-1)

60 El-Maradny, H. A., Mortada, S. A., Kamel, O. A. & Hikal, A. H. 2008 Characterization of ternary complexes of meloxicam-HPβCD and PVP or L-arginine prepared by the spray-drying technique. *Acta Pharm.* **58**, 455–466. (doi:10.2478/v10007-008-0029-9)